Indian Journal of Pure & Applied Physics
Vol. 57, October 2019, pp. 732-736

Fabrication and characterization of thermally oxidized TiO_2 thin films on Si(100) substrates

Umananda M Bhatta[a*], Puspendu Guha[b,c,d], Susheel Kumar G[a] & Nagabharana R M[a]

[a]Centre for Incubation, Innovation, Research and Consultancy, Jyothy Institute of Technology, Bengaluru 560 082, India
[b]Institute of Physics, Sachivalaya Marg, Bhubaneswar 751 005, India
[c]Homi Bhabha National Institute, Training School Complex, Anushakti Nagar, Mumbai 400 085, India
[d]Current Affiliation: RIAM, College of Engineering, Seoul National University, 1 Gwanak-ro, Gwanak-gu, Seoul 08826, Republic of Korea

Received 24 September 2018; accepted 29 April 2019

Mixed phase TiO_2 is known to have better photocatalytic property as the resulting grain boundaries and interfaces between substrate, anatase and rutile phases play a crucial role in transferring/trapping photogenerated electrons. Here we have grown three different thicknesses (10 nm, 30 nm and 50 nm) of Ti thin films on Si(100) substrate in a sputter coater. Thermal oxidation in air at 600 °C for 1 h leads to the formation of mixed phase TiO_2 thin films. Surface morphology and crystalline quality of thin film are discussed using XRD, SEM and TEM results. Moiré fringes resulting from interfacial strain have been discussed using lattice resolved HRTEM images.

Keywords: Thermal oxidation, TiO_2, Mixed phase, HRTEM, Moiré fringes

1 Introduction

TiO_2 is a wide band gap material and has attracted attention as potential solar cell materials (as transparent conducting oxide (TCO)) and also in optoelectronic applications. Its wide gap is dependent on its crystalline structure. Normally, TiO_2 is available in three different phases; anatase, rutile and brukite. Among these, former two are observed in tetragonal structure and the band gap ranging from 3.2 eV to 3.8 eV (both direct and indirect band gap included). Naturally, this large band gap makes sure that it is not optically active in the visible region. In fact, TiO_2/Si is one of the most popular junction materials which are useful in many potential applications including, self-cleaning windows, anti-fogging glasses, gas sensors, self-sterilizing, resistive switching memory device, photodiodes, photocatalysis, and solar cells[1-4]. But the large band gap needs to be tuned more towards visible region and there are number of methods/studies being followed on this front. Among them are injection, doping and hetero junction of TiO_2 with other suitable materials so that the overall band gap could be brought down[5-7]. TiO_2 as a photovoltaic material helps in electron injection and easy transport of photo generated electrons by blocking the holes which results in higher solar efficiency. Creating a heterojunction of TiO_2 with another suitable material like Si helps in achieving this goal.

TiO_2/Si heterojunction could be achieved by several methods including sol-gel method[8,9], chemical vapour deposition[10-12], atomic layer deposition[13], pulsed laser deposition (PLD) [14], RF magnetron sputtering[15,16], and spin coating[17]. Here, to begin with Ti thin films were deposited on Si(100) substrates and then were thermally oxidized in air to get mixed phase TiO_2 thin films. Later we investigate the effect of thickness of TiO_2 thin film on its crystallinity using X-ray diffraction (XRD) and selected area electron diffraction (SAED) techniques. Microstructural characterization and morphological studies are done by using scanning electron microscopy (SEM) and transmission electron microscopy (TEM) techniques.

2 Experimental Details

2.1 TiO_2 deposition

Si(100) substrates were cut into appropriate sizes and cleaned using RCA process. Initially deionized water, NH_4OH (SDFCL) and H_2O_2 (Fisher Scientific) were taken in the ratio of 5:1:1 and was heated upto 75 °C. Si substrate was immersed in this solution for 15 min which removes most of the organic impurities from the surface. Subsequently, the Si substrate was immersed again in a mixture of deionised water, HCl (SDFCL) and H_2O_2 in the ratio of 5:1:1 at 75 °C for

*Corresponding author (E-mail: umananda.b@ciirc.jyothyit.ac.in)

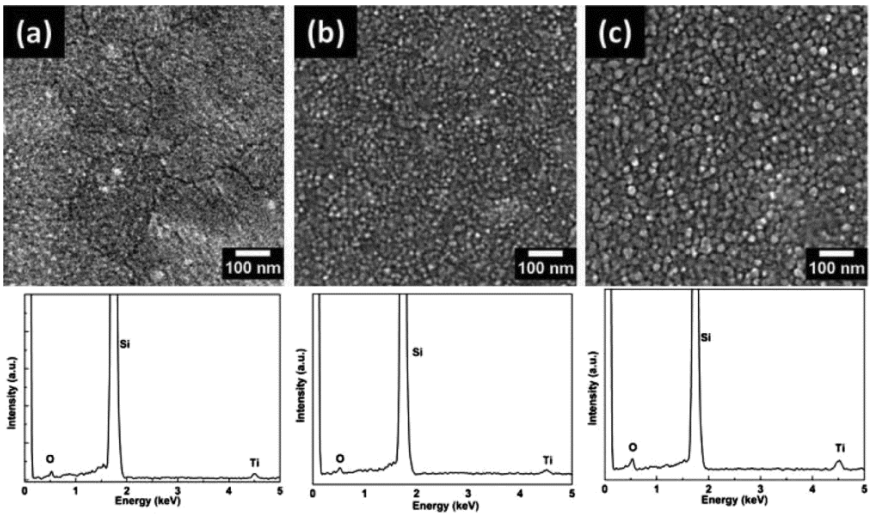

Fig. 1 — Scanning electron micrographs showing surface morphology of TiO_2 thin films of (a) 10 nm, (b) 30 nm and (c) 50 nm thicknesses. Corresponding EDX spectra are also given.

15 min, which removes the metal ions present on the surface, if any. Titanium was deposited using BT300 HHV bench top sputter coating system on cleaned Si(100) wafers. The chamber was maintained at a pressure of 8×10^{-5} mbar initially. During the deposition the pressure was around 4.4×10^{-3} mbar. The deposition time was varied to get thin films of different thicknesses, viz: 10 nm, 30 nm and 50 nm. Later each of these thin films were thermally oxidised in a tubular furnace by passing air with a flow rate of 75 sccm for 1 h which at 600 °C.

2.2 Characterization

X-ray diffraction (XRD) measurements were done in a D8 Advance Eco Powder XRD system with Cu-K_α source. SEM measurements were done in a Neon 40 cross-beam system (M/S Carl Zeiss GmbH) with 20 keV electrons. Planar specimens for TEM measurements were prepared using standard mechanical route where in, TiO_2/Si (100) sample was cut into 3 mm disc using ultrasonic disc cutter and later polished using polisher and dimple grinder. Resulting specimen was subjected to Argon ion milling (3 keV) to reach electron transparency. High resolution transmission electron microscopy (HRTEM) was performed with 200 keV electrons (JEOL UHR JEM-2010).

3 Results and Discussion

Figure 1 shows surface morphology of TiO_2 thin films of three different thicknesses. Lowest thickness shows flat continuous structure with a few prominent cracks. The grains encapsulated by theses cracks are rather large in area indicating better crystalline quality among individual grains. This is also confirmed by TEM studies later (Fig. 2). As the thickness increases, number

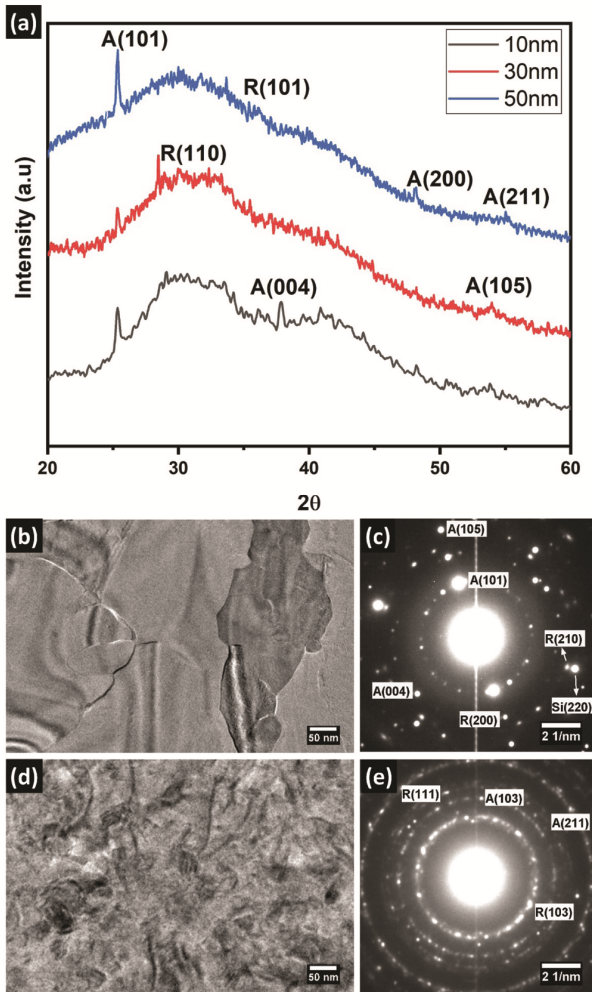

Fig. 2 — (a) XRD data of 10, 30 and 50 nm TiO_2 thin films altogether. (b) and (d) Low magnification TEM images of 10 nm and 50 nm TiO_2 respectively. (c) and (e) show corresponding SAED patterns.

of clusters per unit area increases. There is also an apparent increase in surface roughness. At the highest thickness, grain boundaries are synonymous with individual crystals (which are still attached to each other). Because of enhanced roughness, they appear to be uniformly distributed 20-30 nm sized nanoparticles. Energy dispersive X ray spectra show presence of titanium and oxygen as expected. Si peak comes from the substrate.

Crystalline nature of the thin films was investigated using X-ray diffraction. Figure 2 (a) shows X-ray diffractograms of 10, 30 and 50 nm TiO_2 thin films plotted together. It can be clearly seen that only the anatase peaks (101), (004) and a very weak broad (105) are visible. Among them, (101) is the narrow and strongest (PCPDF 00-021-1272), which suggests that the thin film is fairly oriented in a particular direction. This is also confirmed by low magnification bright field TEM image of 10 nm TiO_2 thin film. Figure 2 (b) shows only a few grains with clear grain boundaries in an approximate area of 0.28 μm^2. Even contrast can be seen within each grain, suggesting that each grain is single crystalline. Corresponding high resolution image Fig. 3 (a) shows a well resolved lattice image of an individual single crystalline grain showing A(101) fringes. CH Kao *et al.*, had studied the transformation of Ti thin film to anatase TiO_2 by a two-stage thermal oxidation[18]. The authors had used much lower temperatures and the substrate was NaCl. But in our case on a Si(100) substrate, 600 °C thermal oxidation in air gives a mixed phase material.

Coming back to XRD for 30 nm thin film (see Fig. 2 (a)), anatase (101) reduces in intensity and corresponding (004) completely disappears. A weak rutile (110) appears now suggesting a slow phase transition with increased thickness (PCPDF 00-021-1276). At the highest thickness (50 nm), couple of additional anatase peaks appear and the (101) becomes more prominent. Spectrum includes a couple of weak rutile peaks as well, suggesting multiple grains of smaller sizes and different orientations. TEM image also confirms the same with several random diffraction contrasts, which are due to polycrystalline nature of the film. Figure 3 (b) is a HRTEM image of 50 nm film. Size of the captured area is same as that of 10 nm film (Fig. 3 (a)), but here it has multiple grains. Grain boundaries are marked with white dotted lines. Each individual grain is single crystalline, albeit of smaller size as compared to that of 10 nm film. So, it gives polycrystalline texture to the film.

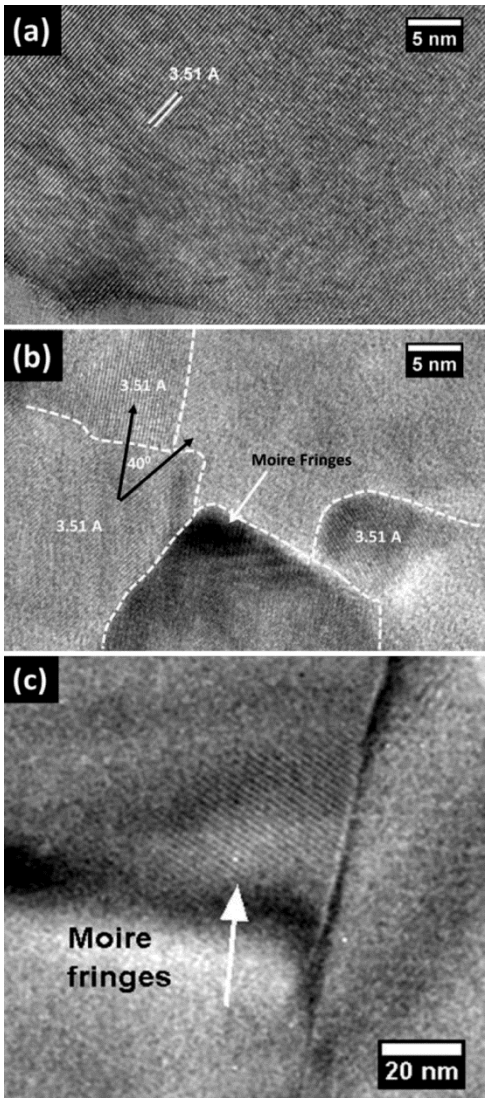

Fig. 3 — (a) and (b) HRTEM images of 10 nm and 50 nm TiO_2 samples and (c) HRTEM image of TiO_2, showing Moiré fringe.

Crystalline quality is further confirmed by selected area diffraction patterns. Figure 2 (c) shows semi-single crystalline diffraction pattern with only a limited number of reflections corresponding to both anatase and rutile phases of TiO_2. Orientational relationship between anatase and underlying Si substrate can also be seen (shown by arrow mark). As shown in Fig. 2 (c), (210) reflection due to Rutile TiO_2 is epitactic with substrate (220) reflection. Figure 2 (e) shows polycrystalline rings for 50 nm thin film, complementing both SEM and XRD observations. Here also we see a mixed phase of rutile and anatase. Even though pure single phase TiO_2 has been studied rigorously on a fundamental level, mixed phase materials are known to display a much higher

level photocatalytic activity[19]. In plane epitactic relationship between individual grains of different phases may also lead to interfacial strain which leads to changing optical band gaps[20]. *David et al.*, have demonstrated that, due to band alignment between anatase and rutile phases, with anatase having higher electron affinity (work function), robust separation of photo-excited charge carriers among two phase occurs, which leads to improved photocatalytic activity[21]. In such materials interface (or grain boundaries in our case) of two different materials or two different phase plays a crucial role. In other words, electrical transport properties in energy storage devices depends majorly on its crystalline properties. It has been shown that, further annealing leads change in optical band gap which helps in hole blocking ability of the thin film.[22] So, fundamental study of such interfaces become even more important as these are the locations where transfer/trapping of photogenerated electrons takes place.

During the deposition, atoms/atomic clusters impinging on the substrate try to diffuse on the surface and settle at a minimum energy location. If the deposition is stopped at an earlier stage (low thickness), the clusters have both time and space and the relationship with the substrate is also maximum at this stage as they are more closer to the substrate. As the thickness increase, more and more clusters fall on the substrate or on the already deposited materials. Number of nucleation centres also increase. This can give rise to two independent/simultaneous scenarios. (i) Competition among more number of nucleation centres will decrease average grain size. Also, these grains are oriented in random directions with respect to one another leading to formation of planar defects like twin boundaries. Figure 3 (b) clears shows this phenomenon with increased number of grains per unit area. (ii) Second scenario will be overlapping of these grains leading to the formation of Moiré fringes. Theoretically, for general Moiré fringes, spacing can be determined using the formula[23]:

$$d_m = \frac{d_1 d_2}{((d_1 - d_2)^2 + d_1 d_2 \beta^2)^{1/2}}$$

where d_1 and d_2 are participating lattice planes and β is the angle between them. Moiré fringes can be of two types, namely translational and rotational. In our case, rotational Moiré fringes are quite possible as shown in Fig. 3 (b). Two grains are at an angle of about 40 degree and the resulting Moiré fringes (shown by arrow) is having a spacing of about ~0.419 nm. Using the above formula, $d_1 = d_2 = 0.35$ nm, $\beta = 0.69$ radians, calculated value of ~0.423 nm. Similarly, another set of Moiré fringes with even larger spacing (~1.69 nm) are shown Fig. 3 (c).

4 Conclusions

TiO_2 thin films of three different thicknesses were fabricated by thermal oxidation of sputtered Ti thin films. With increase in thickness, number of grains per unit area increases and the specimen turns from semi-single crystalline to a poly crystalline in nature. XRD and SAED results reveal that the formed TiO_2 is a mixture of both anatase and rutile. HRTEM images confirm the formation of Moiré fringes due to overlap of multiple grains and the substrate. In the case of lower thickness film, overlaying seems to maintain epitactic relationship at certain orientations with substrate.

Acknowledgement

This project is funded by SERB-DST, Young Scientist grant No YSS2014/000155. Corresponding author would like to thank Prof P V Satyam, Institute of Physics, Bhubaneswar for helping in electron microscopy measurements.

References

1 Kwon D H, Kim K M & Jang J H, *Nat Nanotechnol*, 5 (2010) 148.
2 Maeda M & Watanabe T, *Surf Coat Technol*, 201 (2007) 9309.
3 Karunagaran B, Kim K & Mangalaraja D, *Sol Energy Mater Sol Cells*, 88 (2005) 199.
4 Varghese O K, Gong D & Paulose M, *Sens Actuators B Chem*, 93 (2003) 338.
5 Hendi A A & Yakuphanoglu, *J Alloy Compd*, 665 (2016) 418.
6 Alamgir, Khan W & Ahmad S, *Opt Mater*, 38 (2014) 278.
7 Chandiran A K, Jalebi M A, Nazeeruddin M K & Gratzel M, *ACS Nano*, 8 (2014) 2261.
8 Legrand-Buscema C, Malibert C & Bach S, *Thin Solid Films*, 418 (2002) 79.
9 Aksoy S & Caglar Y, *J Alloy Comp*, 613 (2014) 330.
10 Byung-Chang K, Soon-Bo L & Jin-Hyo B, *Surf Coat Technol*, 131 (2000) 88.
11 Dong H L, Yong S C & Woul I Y, *Appl Phys Lett*, 66 (1995) 815.
12 Sahasrabudhe G, Rupich S M & Jhaveri J, *J Am Chem Soc*, 137 (2015) 14842.
13 Chang Y H, Liu C M & Tsang Y C, *Nanotechnology*, 21 (2010) 225602.
14 Hua L, Guang Y & Aiping C, *Thin Solid Films*, 517 (2008) 745.
15 Cheol H H, Soon-Bo L & Jin-Hyo B, *Thin Solid Films*, 475 (2005) 183.

16 Kaczmarek D, Domaradzki J & Prociow E L, *Opt Mater*, 31 (2009) 1337.
17 Ji T, Cao Y & Peng X, *Appl Surf Sci*, 449 (2018) 358.
18 Kao C H, Yeh S W & Huang H L, *J Phys Chem C*, 115 (2011) 5648.
19 Li G & Gray K A, *Chem Phys*, 339 (2007) 173.
20 Miao L, Jin P & Kaneko K, *Appl Surf Sci*, 212 (2003) 255.
21 Scanlon D O, Dunnill C W & Buckeridge J, *Nat Mater*, 12 (2013) 798.
22 Singh R, Kumar M & Saini M, *Appl Surf Sci*, 418 (2017) 225.
23 Williams D B & Carter C B, *Transmission Electron Microscopy A Textbook for Materials Science*, (Springer Science, Business Media, New York), (2009) 393.